

Attribution of the July 2021 Record-Breaking Northwest Pacific Marine Heatwave to Global Warming, Atmospheric Circulation, and ENSO

Delei Li, Yang Chen, Jifeng Qi, Yuchao Zhu,
Chunhui Lu, and Baoshu Yin

AFFILIATIONS: Li, Qi, and Zhu—CAS Key Laboratory of Ocean Circulation and Waves, Institute of Oceanology, Chinese Academy of Sciences, and Pilot National Laboratory for Marine Science and Technology (Qingdao), Qingdao, China; Chen—State Key Laboratory of Severe Weather, Chinese Academy of Meteorological Sciences, Beijing, China; Lu—National Climate Center, Laboratory for Climate Studies, China Meteorological Administration, Beijing, China; Yin—CAS Key Laboratory of Ocean Circulation and Waves, Institute of Oceanology, Chinese Academy of Sciences, and Pilot National Laboratory for Marine Science and Technology (Qingdao), Qingdao, and College of Earth and Planetary Sciences, University of Chinese Academy of Sciences, Beijing, China

DOI: <https://doi.org/10.1175/BAMS-D-22-0142.1>

Corresponding author: Baoshu Yin,
bsyin@qdio.ac.cn

Supplemental material: <https://doi.org/10.1175/BAMS-D-22-0142.2>

In final form 21 November 2022

© 2023 American Meteorological Society. This published article is licensed under the terms of the default AMS reuse license. For information regarding reuse of this content and general copyright information, consult the AMS Copyright Policy (www.ametsoc.org/PUBSReuseLicenses).

The 2021 northwest Pacific marine heatwave was favored by the atmospheric and oceanic conditions; changes in the mean climate due to anthropogenic warming made the event 43 times more likely.

In July 2021, the northwest Pacific Ocean (NWP) experienced a record-breaking marine heatwave (MHW), featuring SST anomalies larger than 4°C in some coastal areas of the Japan (East) Sea and Okhotsk Sea relative to 1982–2011 (Fig. 1a). This event triggered an unprecedented widespread outbreak of harmful algae in the coastal waters, causing serious damage to the marine ecosystems (Kuroda et al. 2021, 2022) and a record-breaking loss of over 8.19 million U.S. dollars to Japanese coastal fisheries (Iwataki et al. 2022). The MHW might have also contributed to the exceptional humid-hot weather experienced by Japan during the Olympic Games (Sealy and Wang 2021).

Several processes may have contributed to the July 2021 northwest Pacific MHW. Anthropogenic warming has contributed to the increasing occurrences of MHW in recent decades (Hayashi et al. 2021; King et al. 2017; Laufkötter et al. 2020; Oliver et al. 2018b). Natural variability can play a role as well (Oliver et al. 2018a). Anomalies of the 500-hPa geopotential height (z500)

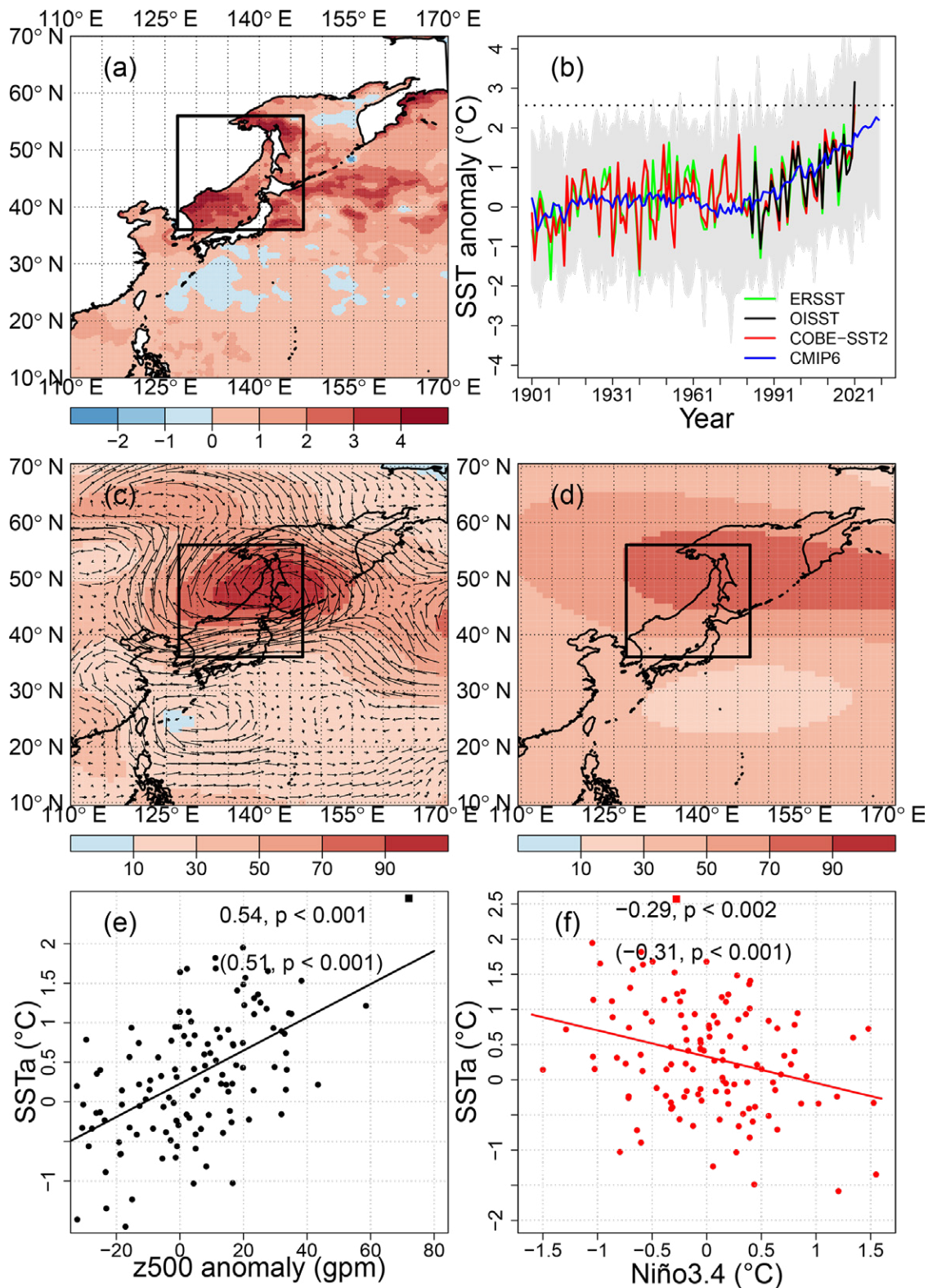


Fig. 1. (a) OISST temperature anomalies in July 2021 over the NWP relative to the July mean of 1982–2011. (b) Time series of July SST anomalies (SSTa) over the study region [black rectangle in (a)] from three observations (ERSSTv5, OISST, and COBE-SST2), CMIP6 ALL simulations (gray shaded) and their ensemble mean (blue line). (c) Observed anomalies of z500 and wind vectors in July 2021. (d) The July anomaly of z500 for the ensemble mean of ALL_high samples. Scatterplots of July SSTa over the study region [black rectangle in (a)] from COBE-SST2 with observed (e) z500 anomaly and (f) Niño-3.4 index. Linear fits are displayed together with correlation coefficients and significance levels calculated before and after detrending, with the latter in parentheses. The square symbols in (e) and (f) indicate the case of July 2021. Note that the anomalies are relative to July mean of 1901–30 except in (a).

show the dominance of an anomalously anticyclonic circulation over the study domain in July 2021 (Fig. 1c). This anticyclonic cell was embedded in a circumglobal Rossby wave train (Fig. ES1a in the online supplemental material; <https://doi.org/10.1175/BAMS-D-22-0142.2>), which might cause hemispheric synchronized land and ocean heatwaves at midlatitudes (Christidis and Stott 2022; Kornhuber et al. 2020; Wehrli et al. 2020). The large-scale SST anomaly pattern features a developing La Niña phase, which was initiated in August 2020, weakened in late spring and summer 2021, and restrengthened to April 2022 (Fig. ES1b). The developing phase of La Niña is also believed important to shape both terrestrial and marine heatwaves in this region (Hong et al. 2001; Takahashi et al. 2016).

This paper mainly aims to answer three questions: 1) What does the July 2021 MHW in the NWP look like in a historical context? 2) What are the relative roles of anthropogenic forcing, atmospheric circulation, and ENSO on the likelihood of the event? 3) Is such an event more likely under an anticyclonic circulation pattern and a developing La Niña phase?

Data and methods

The July 2021 MHW was bounded by 36°–56°N, 127°–147°E over the NWP (Fig. 1a). Considering the observation uncertainty, three observation datasets are used to analyze the long-term variations of July SST over the study domain (Fig. 1b). These datasets include the 0.25° daily NOAA OISST dataset in 1982–2021 (Reynolds et al. 2007), 2.0° monthly NOAA ERSSTv5 in 1901–2021 (Huang et al. 2017), and 1.0° monthly COBE-SST2 in 1901–2021 (Hirahara et al. 2014). We define all anomalies relative to a baseline period 1901–30, which is closer to the preindustrial climate and accounts for most of the anthropogenic effect (Christidis and Stott 2022).

For comparison (Fig. 1b), the OISST July anomaly is calculated relative to the period 1982–2011, we further offset by the mean warming from 1901–30 to 1982–2011 calculated from COBE-SST2 (+0.484°C), to reference it to the chosen base period 1901–30 (e.g., Oliver et al. 2018a).

To analyze the anomalous synoptic pattern during the event (Fig. 1c), z500 and wind components from NOAA-20CrV3 (Slivinski et al. 2019) in 1901–2015 were used, with an extension to 2021 using ERA5 reanalysis (Hersbach et al. 2020) by reconciling their 1979–2015 climatological means (Zhou et al. 2021).

Ten CMIP6 models (Eyring et al. 2016) are evaluated and these runs that can capture the observed probability distribution of July SST anomalies and z500 anomalies (rectangle region in Fig. 1c), Niño-3.4 index, and the relationship between July SST anomalies and z500 anomalies/Niño-3.4 index are selected (see online supplement for simulations evaluation and selection). This results in 54 runs for historical all-forcing (natural plus all anthropogenic forcing) (ALL) and 36 runs for natural-only forcing without the anthropogenic effects (NAT). Since the CMIP6 historical runs terminate at the end of 2014, the historical runs were extended to 2030 with the shared socioeconomic pathway 370 scenarios (SSP370) runs. The data over July 2011–30 are then used as samples, representing current climate conditions similar to July 2021. This generates 1,080 samples (20 years × 54 runs) for ALL experiment. The corresponding 36 natural-only forcing simulations (NAT) from CMIP6 models were selected from 1991 to 2020, which gives 1,080 samples (30 years × 36 runs) as well. The CMIP6 NAT runs end in 2020; considering the general stationary, a longer period for NAT runs can provide a more robust estimation of small probability (Kirchmeier-Young et al. 2021). For consistency, observation and model data were bilinearly remapped onto 1.0° × 1.0° grids with anomalies relative to 1901–30 mean.

We stratify the ALL and NAT samples by their resemblance of large-scale atmospheric circulation to the observed pattern (black rectangle in Fig. 1c), into high resembling ($r > 0.5$) samples ALL_high ($n = 307$), NAT_high ($n = 239$), and low resembling ($r < 0.1$) samples ALL_low

($n = 548$), NAT_low ($n = 574$). Figure 1d shows the anomaly of z500 for the ensemble mean of ALL_high samples, which displays an anticyclone circulation pattern similar to July 2021 (Fig. 1c). El Niño (La Niña) is defined as when the July SST anomaly (calculated relative to a 30-yr running mean) in the Niño-3.4 region (5°N–5°S, 170°–120°W) is greater (less) than 0.5°C (<http://bmcnoldy.rsmas.miami.edu/tropics/oni/>), which generates July SST anomaly samples in different ENSO phases for ALL: ALL_El Niño ($n = 289$), ALL_La Niña ($n = 270$), and ALL_Neutral ($n = 521$).

The exceeding probabilities were obtained using the generalized Pareto distribution if the threshold lay at the tails of the distribution (Christidis and Stott 2022; Lu et al. 2020). The fraction of attributable risk ($\text{FAR} = 1 - P_0/P_1$) and the corresponding risk ratios ($\text{RR} = P_1/P_0$) (Chen et al. 2019; Fischer and Knutti 2015) were used to estimate the effect of anthropogenic influence, atmospheric circulation, and ENSO on the present-day likelihood of the July 2021 MHW in the NWP. For instance, to quantify the anthropogenic influence, P_0 and P_1 indicates the probabilities exceeding the threshold for the NAT and ALL samples, respectively. The RR describes how much more or less likely the event is in the ALL samples with anthropogenic influence compared to NAT samples without anthropogenic influence. FAR is interpreted as the fraction of the likelihood of an event that is attributable to the anthropogenic influence. E.g., at $\text{RR} = 5$ (with $\text{FAR} = 0.8$), the likelihood of an event occurring under the anthropogenic influence is 5 times that of its occurring without anthropogenic influences, and anthropogenic influence explains 80% attributable risk for the event. Furthermore, a Monte Carlo bootstrap was performed 1,000 times to estimate the uncertainty of FAR and RR by randomly resampling (Christidis et al. 2013).

Results

In July 2021, almost the entirety of the study domain features positive SST anomalies relative to the period 1982–2011, with 59.3% of the region having the record-breaking July SST (Fig. 1a). In terms of domain-averaged values, July 2021 is the warmest one among all historical July counterparts for all three observations, with anomalies of 3.16°, 2.57°, and 2.40°C for OISST, COBE-SST2, and ERSSTv5, respectively. The anomalies of the COBE-SST2 dataset are used hereafter and 2.57°C is used as the threshold to characterize the July 2021 MHW, due to it having a comparable resolution to CMIP6 models (Table ES1) and its SST anomaly in July 2021 is closer to the ensemble mean of observations. It is found that the selected CMIP6 ALL models can capture the long-term trends of SST, z500, and Niño-3.4 index, and the observation variations are encapsulated by the spread of CMIP6 runs (Fig. 1b, Figs. ES1c,d).

MHWs are typically driven by heat transport by ocean currents, persistent large-scale atmospheric synoptic systems, and large-scale climate modes (Sen Gupta et al. 2020). Specific to this case, a strong anomalous anticyclonic circulation was centered over the NWP (Fig. 1c), associated with a northwestward expansion of the North Pacific subtropical high (Kuroda and Setou 2021), facilitating increased surface solar radiation and adiabatic heating, and further warming up the upper ocean through air–sea interactions. The July SST anomalies show a statistically significant positive correlation ($R = 0.54$) with the z500 anomaly in this region (Fig. 1e) and a significant negative correlation ($R = -0.29$) with the Niño-3.4 index (Fig. 1f).

The likelihood of July 2021 MHW is fairly rare (0.48%) in the NAT world (Fig. 2a and Table 1). It is found that human influences increased the likelihood by 42.87 times and explained 97.7% (90% CI: 96.2%–99.1%) attributable risk for the record-breaking July 2021 MHW (Figs. 2a,e, Table 1). The return period (inverse probability) is estimated to decrease from more than two centuries in the NAT world to about 5 years in the present climate (Table 1). The results are generally consistent with those findings of Laufkötter et al. (2020), indicating the significant role of anthropogenic forcing on the likelihood of MHW.

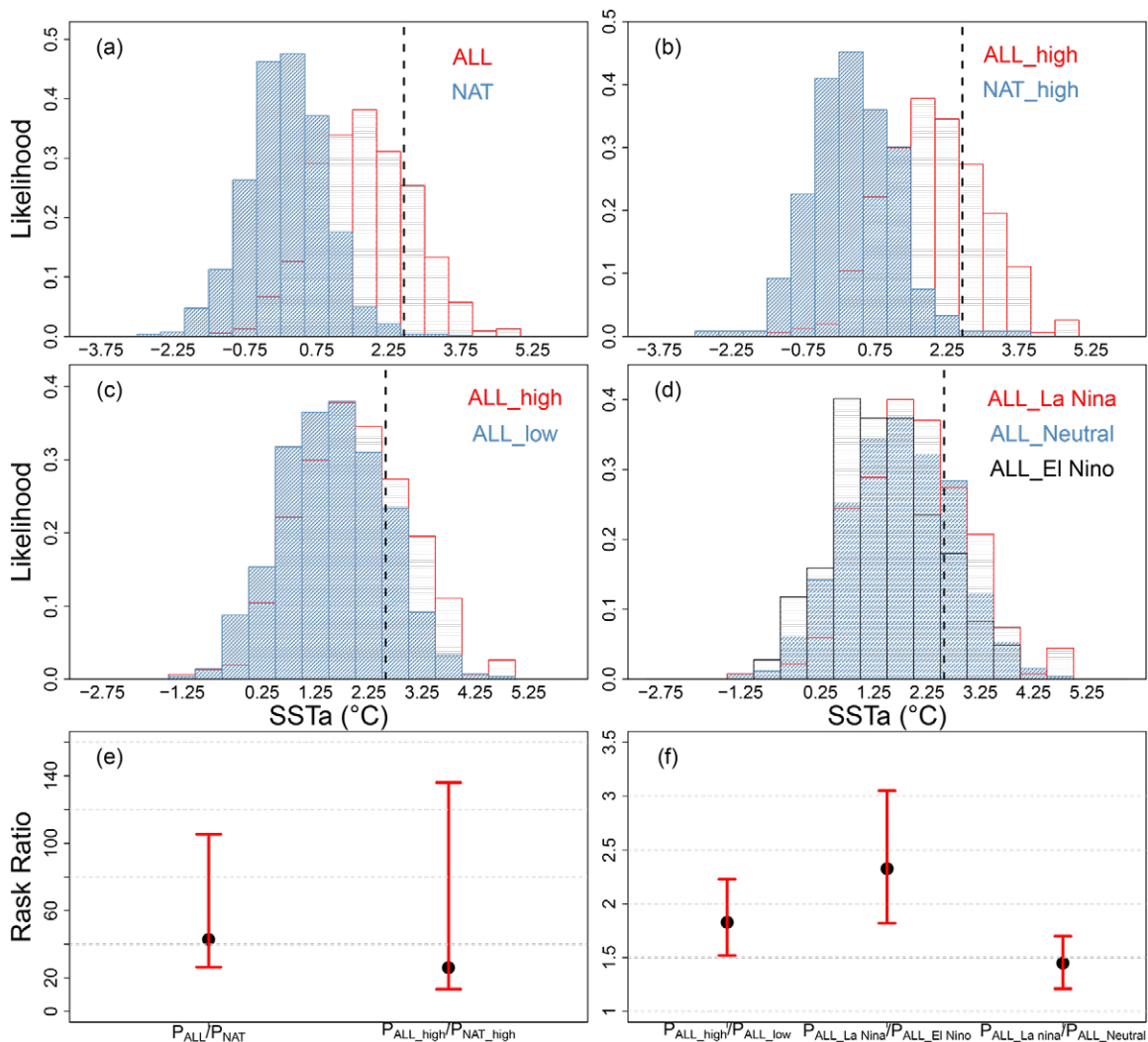


Fig. 2. (a) Normalized distributions of the July SST anomaly for CMIP6 ALL and NAT cases. (b) As in (a), but only for cases with similar circulation patterns (within the black rectangle in Fig. 1c) to that in July 2021 with (red, ALL_high) and without (blue, NAT_high) anthropogenic forcing. (c) As in (a), but only for CMIP6 "All" cases with high (red, ALL_high) and low (blue, ALL_low) correlations with the flow pattern (within the black rectangle in Fig. 1c) in July 2021. (d) As in (a), but only for cases under the conditions of El Niño, neutral, and La Niña. (e),(f) Best estimates (black points) and 90% confidence intervals (red whiskers) of the risk ratio for different groups of cases from (a)–(d).

Table 1. The best estimate and 90% confidence intervals (90% CI) of the return period (RP; years), the fraction of attributable risk (FAR), and risk ratio (RR) estimated with CMIP6 models.

Runs	RP (90% CI)	FAR (90% CI)	RR (90% CI)
ALL	4.88 (4.51, 5.29)	0.977 (0.962, 0.991)	42.87 (26.3, 105.4)
NAT	209.00 (130, 501)		
ALL_high	3.55 (3.16, 4.03)	0.962 (0.924, 0.993)	26.09 (13.2, 136)
Nat_high	92.51 (48, 502)		
ALL_high	3.55 (3.16, 4.03)	0.455 (0.344, 0.552)	1.83 (1.52, 2.23)
ALL_low	6.51 (5.69, 7.48)		
ALL_La Niña	3.39 (3.02, 3.98)	0.57 (0.449, 0.672)	2.33 (1.82, 3.05)
ALL_El Niño	7.90 (6.6, 10)		
ALL_La Niña	3.39 (3.02, 3.98)	0.31 (0.171, 0.413)	1.45 (1.21, 1.7)
ALL_Neutral	4.92 (4.4, 5.51)		

In terms of conditional attributions based on the high-correlation samples (ALL_high and NAT_high), we find again that human influence shifts the distribution to warmer temperatures (Fig. 2b), making the event 26.09 times more likely to occur and explained 96.2% (90% CI: 92.4%, 99.3%) attributable risk for the event (Figs. 2b,e, Table 1). The return period (3.55 years) is lower in the conditional attribution compared to the unconditional attribution since anticyclonic conditions favor warm anomalies.

We also compared the likelihood of the event between anticyclonic conditions compared to other circulation patterns under the present-day climate, by using the ALL_high and ALL_low samples. It is estimated that anticyclonic conditions make the event 1.83 times (90% CI: 1.52–2.23) more likely to occur and explained 45.5% (90% CI: 34.4%, 55.2%) attributable risk for the event (Figs. 2c,f, Table 1). Comparing the all-forcings samples in La Niña years with El Niño (neutral) years, we found that La Niña increased the likelihood by 2.33 (1.45) times and explained 57% (31%) attributable risk (see Figs. 2d,f, Table 1).

In addition, an experimental attribution analysis revealed that the likelihood of detrended SSTa of July 2021 (0.84°C) in the study is comparable between ALL (ALL_high) runs and NAT (NAT_high) runs (Fig. ES2). This gives an estimated risk ratio of 1.04 (90% CI: 0.90, 1.19) and 0.93 (90% CI: 0.74, 1.15) for ALL/NAT and ALL_high/NAT_high, respectively, implying that the detrended SST anomaly cannot be attributed to the anthropogenic forcing.

Conclusions

In July 2021, an unprecedented MHW hit the northwest Pacific Ocean. Attribution analysis based on the CMIP6 models reveals that human influence is estimated to have made such an event about 43 times more likely and to have the return period from more than two centuries in the NAT world to about 5 years in the present climate. The anticyclone atmospheric patterns and developing phase of La Niña favor the likelihood of such an event by a factor of about 2, which is weaker than the anthropogenic influence. In addition, an experimental attribution analysis based on detrended SSTa reveals that the increased likelihood of July 2021 MHW in the NWP is governed by the warming mean climate instead of climatic changes in SST variance.

Acknowledgments. The study was supported by the National Key Research and Development Project of China (2022YFE0112800), the National Natural Science Foundation of China (42176203), the Strategic Priority Research Program of the Chinese Academy of Sciences (XDB42000000), the NSFC-Shandong Joint Fund (U1806227), the Youth Innovation Promotion Association CAS (2022204), and the Taishan Scholars Program (tsqn202211252).

References

- Chen, Y., and Coauthors, 2019: Anthropogenic warming has substantially increased the likelihood of July 2017–like heat waves over central eastern China [in “Explaining Extreme Events of 2017 from a Climate Perspective”]. *Bull. Amer. Meteor. Soc.*, **100** (1), S91–S95, <https://doi.org/10.1175/BAMS-D-18-0087.1>.
- Christidis, N., and P. A. Stott, 2022: Anthropogenic climate change and the record-high temperature of May 2020 in western Europe [in “Explaining Extreme Events of 2020 from a Climate Perspective”]. *Bull. Amer. Meteor. Soc.*, **103** (3), S33–S37, <https://doi.org/10.1175/BAMS-D-21-0128.1>.
- Christidis, N., P. A. Stott, A. A. Scaife, A. Arribas, G. S. Jones, D. Copsey, J. R. Knight, and W. J. Tennant, 2013: A new HadGEM3-A-based system for attribution of weather- and climate-related extreme events. *J. Climate*, **26**, 2756–2783, <https://doi.org/10.1175/JCLI-D-12-00169.1>.
- Eyring, V., S. Bony, G. A. Mehl, C. A. Senior, B. Stevens, R. J. Stouffer, and K. E. Taylor, 2016: Overview of the Coupled Model Intercomparison Project phase 6 (CMIP6) experimental design and organization. *Geosci. Model Dev.*, **9**, 1937–1958, <https://doi.org/10.5194/gmd-9-1937-2016>.
- Fischer, E. M., and R. Knutti, 2015: Anthropogenic contribution to global occurrence of heavy-precipitation and high-temperature extremes. *Nat. Climate Change*, **5**, 560–564, <https://doi.org/10.1038/nclimate2617>.
- Hayashi, M., H. Shiogama, S. Emori, T. Ogura, and N. Hirota, 2021: The northwestern Pacific warming record in August 2020 occurred under anthropogenic forcing. *Geophys. Res. Lett.*, **48**, e2020GL090956, <https://doi.org/10.1029/2020GL090956>.
- Hersbach, H., and Coauthors, 2020: The ERA5 global reanalysis. *Quart. J. Roy. Meteor. Soc.*, **146**, 1999–2049, <https://doi.org/10.1002/qj.3803>.
- Hirahara, S., M. Ishii, and Y. Fukuda, 2014: Centennial-scale sea surface temperature analysis and its uncertainty. *J. Climate*, **27**, 57–75, <https://doi.org/10.1175/JCLI-D-12-00837.1>.
- Hong, C., K.-D. Cho, and H.-J. Kim, 2001: The relationship between ENSO events and sea surface temperature in the East (Japan) Sea. *Prog. Oceanogr.*, **49**, 21–40, [https://doi.org/10.1016/S0079-6611\(01\)00014-3](https://doi.org/10.1016/S0079-6611(01)00014-3).
- Huang, B., and Coauthors, 2017: Extended Reconstructed Sea Surface Temperature, version 5 (ERSSTv5): Upgrades, validations, and intercomparisons. *J. Climate*, **30**, 8179–8205, <https://doi.org/10.1175/JCLI-D-16-0836.1>.
- Iwataki, M., and Coauthors, 2022: Morphological variation and phylogeny of *Karenia selliformis* (Gymnodiniales, Dinophyceae) in an intensive cold-water algal bloom in eastern Hokkaido, Japan. *Harmful Algae*, **114**, 102204, <https://doi.org/10.1016/j.hal.2022.102204>.
- King, A. D., D. J. Karoly, and B. J. Henley, 2017: Australian climate extremes at 1.5°C and 2°C of global warming. *Nat. Climate Change*, **7**, 412–416, <https://doi.org/10.1038/nclimate3296>.
- Kirchmeier-Young, M. C., H. Wan, and X. Zhang, 2021: Anthropogenic contribution to the rainfall associated with the 2019 Ottawa River flood [in “Explaining Extreme Events of 2019 from a Climate Perspective”]. *Bull. Amer. Meteor. Soc.*, **102** (1), S33–S38, <https://doi.org/10.1175/BAMS-D-20-0191.1>.
- Kornhuber, K., D. Coumou, E. Vogel, C. Lesk, J. F. Donges, J. Lehmann, and R. M. Horton, 2020: Amplified Rossby waves enhance risk of concurrent heatwaves in major breadbasket regions. *Nat. Climate Change*, **10**, 48–53, <https://doi.org/10.1038/s41558-019-0637-z>.
- Kuroda, H., and T. Setou, 2021: Extensive marine heatwaves at the sea surface in the northwestern Pacific Ocean in summer 2021. *Remote Sens.*, **13**, 3989, <https://doi.org/10.3390/rs13193989>.
- Kuroda, H., T. Azumaya, T. Setou, and N. Hasegawa, 2021: Unprecedented outbreak of harmful algae in Pacific coastal waters off southeast Hokkaido, Japan, during late summer 2021 after record-breaking marine heatwaves. *J. Mar. Sci. Eng.*, **9**, 1335, <https://doi.org/10.3390/jmse9121335>.
- Kuroda, H., Y. Taniuchi, T. Watanabe, T. Azumaya, and N. Hasegawa, 2022: Distribution of harmful algae (*Karenia* spp.) in October 2021 off southeast Hokkaido, Japan. *Front. Mar. Sci.*, **9**, 841364, <https://doi.org/10.3389/fmars.2022.841364>.
- Laufkötter, C., J. Zscheischler, and T. L. Frolicher, 2020: High-impact marine heatwaves attributable to human-induced global warming. *Science*, **369**, 1621–1625, <https://doi.org/10.1126/science.aba0690>.
- Lu, C., Y. Sun, N. Christidis, and P. A. Stott, 2020: Contribution of global warming and atmospheric circulation to the hottest spring in eastern China in 2018. *Adv. Atmos. Sci.*, **37**, 1285–1294, <https://doi.org/10.1007/s00376-020-0088-5>.
- Oliver, E. C. J., S. E. Perkins-Kirkpatrick, N. J. Holbrook, and N. L. Bindoff, 2018a: Anthropogenic and natural influences on record 2016 marine heat waves [in “Explaining Extreme Events of 2016 from a Climate Perspective”]. *Bull. Amer. Meteor. Soc.*, **99** (1), S44–S48, <https://doi.org/10.1175/BAMS-D-17-0093.1>.
- Oliver, E. C. J., and Coauthors, 2018b: Longer and more frequent marine heatwaves over the past century. *Nat. Commun.*, **9**, 1324, <https://doi.org/10.1038/s41467-018-03732-9>.
- Reynolds, R. W., T. M. Smith, C. Liu, D. B. Chelton, K. S. Casey, and M. G. Schlax, 2007: Daily high-resolution-blended analyses for sea surface temperature. *J. Climate*, **20**, 5473–5496, <https://doi.org/10.1175/2007JCLI1824.1>.
- Sealy, A., and S. Wang, 2021: Heat and humidity make “Tokyo summer the worst in the history of Olympics.” CNN, <https://edition.cnn.com/2021/07/30/sport/tokyo-2020-heat-weather-spt-intl/index.html>.
- Sen Gupta, A., and Coauthors, 2020: Drivers and impacts of the most extreme marine heatwave events. *Sci. Rep.*, **10**, 19359, <https://doi.org/10.1038/s41598-020-75445-3>.
- Slivinski, L. C., and Coauthors, 2019: Towards a more reliable historical reanalysis: Improvements for version 3 of the Twentieth Century Reanalysis system. *Quart. J. Roy. Meteor. Soc.*, **145**, 2876–2908, <https://doi.org/10.1002/qj.3598>.
- Takahashi, C., M. Watanabe, H. Shiogama, Y. Imada, and M. Mori, 2016: A persistent Japanese heat wave in early August 2015: Roles of natural variability and human-induced warming [in “Explaining Extreme Events of 2015 from a Climate Perspective”]. *Bull. Amer. Meteor. Soc.*, **97** (12), S107–S112, <https://doi.org/10.1175/BAMS-D-16-0157.1>.
- Wehrli, K., M. Hauser, and S. I. Seneviratne, 2020: Storylines of the 2018 Northern Hemisphere heatwave at pre-industrial and higher global warming levels. *Earth Syst. Dyn.*, **11**, 855–873, <https://doi.org/10.5194/esd-11-855-2020>.
- Zhou, C., A. Dai, J. Wang, and D. Chen, 2021: Quantifying human-induced dynamic and thermodynamic contributions to severe cold outbreaks like November 2019 in the eastern United States [in “Explaining Extreme Events of 2019 from a Climate Perspective”]. *Bull. Amer. Meteor. Soc.*, **102** (1), S17–S23, <https://doi.org/10.1175/BAMS-D-20-0171.1>.